

# Solar photovoltaic generation for charging shared electric scooters

Rui Zhu<sup>a,b,c</sup>, Dániel Kondor<sup>a,d</sup>, Cheng Cheng<sup>e,\*</sup>,  
Xiaohu Zhang<sup>f</sup>, Paolo Santi<sup>g,h</sup>, Man Sing Wong<sup>b,c</sup>, Carlo Ratti<sup>g</sup>

<sup>a</sup>*Senseable City Laboratory, Future Urban Mobility IRG, Singapore-MIT Alliance for Research and Technology, 1 Create Way, #09-02 Create Tower, Singapore 138062.*

<sup>b</sup>*Department of Land Surveying and Geo-Informatics, The Hong Kong Polytechnic University, Kowloon, Hong Kong, China.*

<sup>c</sup>*Research Institute for Land and Space, The Hong Kong Polytechnic University, Hong Kong, China.*

<sup>d</sup>*Complexity Science Hub, Josefstädter strasse 39 1080 Vienna, Austria.*

<sup>e</sup>*Department of System Science, Institute of High Performance Computing, Agency for Science, Technology and Research (A\*Star), 1 Fusionopolis Way, #16-16 Conneris, Singapore 138632.*

<sup>f</sup>*Department of Urban Planning and Design, The University of Hong Kong, Hong Kong, China.*

<sup>g</sup>*Senseable City Laboratory, Department of Urban Studies and Planning, Massachusetts Institute of Technology, Cambridge MA 02139 USA.*

<sup>h</sup>*Istituto di Informatica e Telematica del CNR, 56124 Pisa, Italy.*

---

## Abstract

Scooter-sharing has been introduced as a new transportation mode. However, e-scooters have a limited battery capacity and require frequent charging, which causes the operational cost significantly high and hinders the viability of the service. To tackle this problem, this study proposes a solar charging solution with the creation of a real-time shareability network that maximizes the scooter-sharing capability and minimizes the total trip distance, constrained by e-scooters with real-time battery levels. Specifically, hourly solar potential is simulated based on a three-dimensional solar irradiation model so that photovoltaic (PV) electricity generation can be estimated when PV modules are installed at the parking stations, which enables solar charging when the origin-destination matrix of scooter-sharing trips is clustered and associated to the charging stations. As a case study in Singapore, the proposed solar charging system only needs 1-3 m<sup>2</sup> PV modules at each station and 24%-67% of the total number of e-scooters to support almost all the real trips with a 98% reduction of trips used for charging. The system also supports 90% of on-demand mobility for at least three consecutive days without solar charging, which suggests the resilience of the system and inspires us to promote the proposed solar charging in the other global cities.

**Keywords:** Solar energy; Solar charging; Building integrated photovoltaics;  
Scooter-sharing; Shareability network; Geographical information science

---

\*Corresponding author. Email: cheng\_cheng@ihpc.a-star.edu.sg

## 1. Introduction

### 1.1. Background and motivation

Nowadays, transportation consumes a substantial amount of energy that made air pollution severe and the urban heat island phenomenon prominent [1, 2]. To alleviate the increasing pressure on environmental protection and traffic demand, electric vehicles with on-demand mobility options (e.g., car-sharing [3], ride-hailing [4, 5] and ride-sharing [6, 7]) are explosively being developed. Simultaneously, shared electric scooters are increasingly being used for serving the first- and last-mile trips [8, 9]. However, due to the limited battery capacity, the shared e-scooters usually need crowdsourcing suppliers for frequent charging, which significantly hinders the availability of the scooter-sharing service.

One study reported that 31.60% and 7.87% of the total scooter-sharing trips in two discrete areas in Singapore in February 2019 were driven by the charging purpose [10]. As a result, the operators need to perform regular charging of the e-scooters since their battery capacity severely constrains the travel range to only a few kilometers [11]. Although the cost of the electricity itself is cheap as e-scooters usually consume little energy, the manpower costs of performing charging can be significant. For instance, scooter-sharing company Lime pays between \$5 and \$12 per scooter for independent contractors to perform charging [12] and Bird pays between \$5 and \$25 for each in the US [13]. Consequently, charging e-scooters has become a cut-throat business for scooter-sharing service [14].

To tackle this problem, one possible solution is to construct photovoltaic (PV) platforms at the parking stations to provide solar charging service, which has been proposed and developed by many studies for charging electric vehicles [11], with a focus of system design [15], temporal city-scale matching [16], environmental and economic analysis [17], and grid operation [18]. These studies suggested that solar PV modules installed at an optimized location and size could provide a reasonable amount of electricity. Compared to the traditional charging method relying on crowdsourcing suppliers or logistical vehicles, this solution provides solar charging when scooters are idle at the stations so that the availability of the scooters will not be influenced.

Others studied building-integrated photovoltaics (BIPV) focusing on the optimization of battery storage [19, 20], subsidy strategy [21], and micro-grid operation and control [22].

However, they did not consider the spatial and temporal heterogeneous of solar accessibility constraint in a high density of built environment, which can significantly influence the electricity generation of PV platforms and hence affect real-time solar charging for shared e-scooters. In addition, systematic optimization of the PV size and layout is needed for a set of PV modules to be equipped at the parking stations, which should adapt to a real-time scooter-sharing network to provide an adequate amount of electricity.

Thus, to provide a feasible solar charging service for scooter-sharing, this study aims to design a solar charging system to meet the energy demand of the on-demand mobility, which integrates a real-time estimation of electricity generation for all the PV platforms at the parking stations constraint in a real-time shareability network. Such a solution will allow charging scooters at appropriate times and locations to increase their availability continuously, reduce the need to transport scooters for charging purposes, and thus decrease manpower costs significantly.

## *1.2. Solar irradiation estimation*

Accurately estimating solar PV potential at scooter parking stations is important for integrating an effective estimation of solar charging potential into a dynamic scooter-sharing network. This is because instant weather determines solar potential conclusively [23] and urban morphology alters solar distribution radically [24], thus creating solar accumulative or dispersive regions in a city. In the previous study, estimation of solar potential was mainly focused on four progressive perspectives: (i) investigating the spatial distribution patterns of solar irradiation on urban surfaces [25, 26, 27, 28], (ii) analyzing the changes of solar accessibility on existing buildings when a number of new buildings are built [29], (iii) optimizing solar accessibility by designing new urban forms or hybrid systems [30, 31], and (iv) deep learning and GIS-based estimation of solar PV potential for real electricity demand [32, 33, 34, 35]. Studies relying on existing buildings to estimate solar irradiation has achieved fine spatial resolution [25, 36] and various temporal resolution in seasonal, monthly, or hourly scales [25, 26, 27, 36], which allows an estimation of the spatial distribution of solar irradiation in a built environment. However, it is unclear for these models to handle with complex geometries of buildings (e.g., rooftops are concave polygons and footprints of buildings are nested with each other) and support Big Data computation over a large urban

area, which is vital for this study to equip multiple PV platforms along street canyons in a megacity, such as Singapore.

To obtain an accurate estimation of solar PV potential at all the parking stations, this study will utilize an advanced solar estimation model for solar estimation with high spatio-temporal resolutions, which models solar distribution on 3D urban surfaces comprehensively affected by geo-location (i.e., quantifying direct and diffuse solar irradiation based on the latitude and instant of time), historical weather (i.e., determining near-ground solar irradiation qualified by land cover), and urban morphology (i.e., creating 3D shadow made by all the surrounding 3D buildings) [24]. On this basis, scooters can get a quantified PV charging potential when they park at a station with determined parking duration.

### *1.3. Solar charging for e-vehicles and e-scooters*

Solar charging has three foreseeable advantages, which can be deployed at solar-abundant locations, configured to provide the needed energy throughout the day if supported by storage batteries, and environment friendly [37, 38]. In addition, many studies have suggested that constructing and maintaining such charging stations for electric vehicles is relatively cheap and the payback period only takes a few months [39, 40, 41]. Therefore, it is reasonable to consider that solar charging is capable of charging electric scooters since shared electric scooters are less energy demanding, and utilizing solar charging can potentially cut operational costs with the flexibility of deployment compared to the alternative of connecting to the national grid.

To perform solar charging for electric vehicles, most studies focused on the prediction of PV generation and charging load demand [42, 43, 44], which is important for the electrical system design. In comparison, this study also aims to predict PV generation and charging demand but will emphasize real-time simulation to investigate the feasibility of solar charging for a scooter-sharing system, which has not been studied before. On the other hand, two studies investigated PV charging capability of large parking lots in open space, which suggested that solar electricity could cover 90% of the American public living within 15 miles of a Walmart in the US [45] and the payback time is estimated to be 14 years with the use of smart charging and energy storage in Almada, Portugal [46]. However, for solar charging of scooters which usually travel in street canyons, a fine-scale estimation is needed



by incorporating PV generation into a built environment. Although one study analyzed the energy performance of a roof PV system for charging electric vehicles [17], the proposed standalone electric system did not consider the charging capability for a vehicle-sharing or scooter-sharing network.

Only a few studies particularly investigated the solar charging approach for e-scooters, which developed a sliding mode controller with a boost converter to reduce voltage stresses on the power switch [47], designed solar-powered e-bike charging station by providing alternating current, direct current, and wireless charging [48], and employed a standalone solar PV system with a battery storage [49]. None of these have established a systematic optimization of solar charging adapting to energy demand from a real-time scooter-sharing network.

#### *1.4. Real-time mobility sharing network*

The use of shared vehicles with self-repositioning capabilities (i.e., a form of limited autonomy) has been suggested as an effective way to overcome imbalances in demand that limit utilization of vehicles [50, 51]. Specifically, self-repositioning scooters have been in the driving test phase in Singapore [52], which makes it possible for us to integrate self-repositioning functionality into a real-time shareability network to maximize the capability of solar charging. Therefore, this study can perform two types of estimations on the solar charging potential, based on spatio-temporal analysis of the real-world data of shared scooter usages. First, this study only considers the recorded scooter-sharing trips with a determined number of scooters to estimate the number of trips that could be served if battery charging is solely based on PV modules installed at stations. Second, in a more advanced scenario, this study simulates the operation of a number of scooters with limited autonomy, where repositioning is carried out autonomously, and charging is based on PV modules installed at stations. The second estimation can also minimize the number of operated scooters based on the combination of limited autonomy and solar charging.

With the recent popularity of shared bicycle and scooter systems, there has been considerable interest in their optimization from the research community. Previous studies have dominantly focused on analyzing usage patterns [9, 10, 53, 54, 55], real-time or static trip planning [56, 57, 58, 59], or optimizing rebalancing [60, 61, 62]. In station-based systems, one study also optimized an optimal pair of stations for borrowing and returning for a given trip

demand [63]. While most of the previous studies considered bicycles, some recent studies also focused on the fleet size (i.e., the number of e-scooters) management of autonomous scooters [51, 64]. However, all these studies did not develop a shareability network to dispatch scooters to on-demands in aware of the real-time battery range, which becomes essential to provide a practical solar charging solution for scooter-sharing.

### 1.5. Contribution

To the best of our knowledge, this is the first study to consider dynamic charging based on solar energy in combination with fleet size optimization, and thus provide an important novel contribution to the operational aspects of current and future shared mobility systems. In summary, the main contributions of this study are: (i) *providing* an accurate estimation of solar PV potential in an urban environment to estimate the charging potential at parking stations, (ii) *analyzing* battery usage of e-scooters in real-world conditions, (iii) *estimating* the benefit of solar charging based on the current fleet size of scooters, and (iv) *simulating* a hypothetical fleet size with limited autonomy and evaluate the potential additional benefits of solar charging in this context.

The rest paper is organized as follows. Section 2 proposes a solar charging framework with an integration of a shareability network. Section 3 introduces the study area, the dataset, and the system implementation. Section 4 presents an analysis of battery usage based on the recorded scooter-sharing data. Section 5 demonstrates an analysis of solar charging based on the operated scooters. Section 6 presents an analysis of solar charging for a variable number of scooters with self-repositioning functionality. Finally, Section 7 makes a discussion and conclusions.

## 2. Solar PV charging framework for scooter-sharing

This study proposes a solar PV charging framework with three hierarchical modules (Figure 1). The first module estimates solar irradiation on 3D urban surfaces at the fine spatio-temporal resolution, the second module estimates real-time battery capacity of all the e-scooters based on their status and the PV electricity generation with determined PV layouts, and the third module develops a battery-aware real-time shareability network to provide an energy-efficient scooter-sharing service. The nomenclature is listed in Table 1.

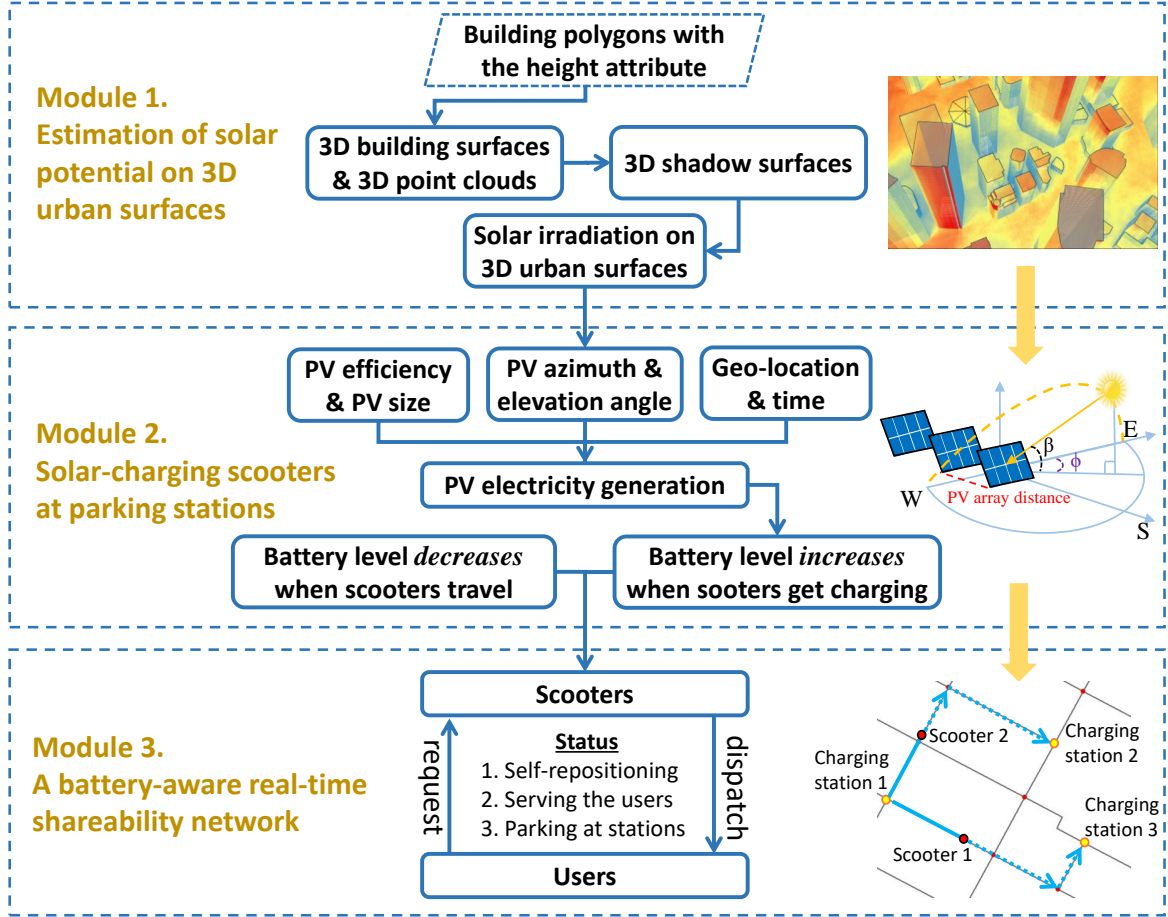


Figure 1: A solar PV charging framework integrated with a real-time shareability network.

### 2.1. Estimation of solar potential on 3D urban surfaces

This study utilizes an established model to accurately estimate solar potential on three-dimensional (3D) urban surfaces at an instant of time, including rooftops, façades, and ground [24]. The model quantifies the effects of geo-location (i.e., the latitude of a city), urban morphology (i.e., 3D shadow surfaces created by *all* the 3D buildings), and historical weather (i.e., cloud cover quantified by diffuse proportion and transmissivity that determines direct and diffuse irradiation) on solar distribution. It even supports complicated building geometries when the footprints of buildings are concave polygons or when the footprints are nested with each other. At the same time, 3D urban surfaces are represented by 3D cloud points of irradiation with a constant spatial resolution at  $s$  m, which means that each point takes an area of  $s \times s$  m<sup>2</sup> with determined solar irradiation. Based on this, 3D solar radiation vectors from a particular elevation angle  $\alpha$  and azimuth  $z$  pass through the atmosphere and intersect on 3D urban surfaces, resulting in the creation of 3D shadow surfaces. As such, locations below the shadow surfaces are in shadow versus other locations that are in light and will be updated with the estimated solar potential. Thus, for each parking station with accurate location information, the solar potential for a series of consecutive periods can be estimated when the PV layout is determined.

Table 1: Nomenclature for solar PV charging of e-scooters.

No.	Abbre.	Meaning
1	$s$	spatial resolution of 3D point clouds
2	$\delta_d$	diffuse proportion
3	$\delta_t$	transmissivity
4	$\alpha$	elevation angle of solar irradiation
5	$z$	azimuth of solar irradiation
6	$u$	direct and diffuse solar irradiation
7	$e$	generated PV electricity
8	$i$	solar charging station ID
9	$a$	PV area at each solar charging station
10	$t$	parking period of an e-scooter at a station each time
11	$o$	departure location of a reserved trip
12	$d$	arrival location of a reserved trip
13	$t_r$	an instant of reservation time
14	$c$	current location of a scooter
15	$e_t$	the total battery needed to serve a trip
16	$e_c$	the remaining battery of a scooter
17	$d_t$	the total distance of a planned trip
18	$d_c$	the traveled distance of a planned trip
19	$sp$	the shortest path from $o$ to $d$
20	$cap$	the full battery capacity of an e-scooter
21	$n$	the fleet size of the e-scooters
22	$r$	record of a reservation
23	$s$	record of an e-scooter
24	$p$	record of a planned trip
25	$\mathcal{R}$	a complete set of reservations
26	$\mathcal{S}$	a complete set of e-scooters
27	$\mathcal{P}$	a complete set of planned trips
28	$O_s$	a set of scooters parking at the stations
29	$O_o$	a set of scooters parking outside the stations
30	$O_t$	a set of scooters serving trips or making repositioning
31	$R$	a set of received reservations during each period
32	$R_s$	a set of served reservations in $R$
33	$R_u$	a set of unserved reservations in $R$

The Sun Earth Tool is used to compute  $\alpha$  and  $z$  of solar radiation at an instant of time  $t'$  and location  $l$  [65]. Since cloud influences direct and diffuse solar irradiation ( $u$ ) significantly, hourly cloud-cover data for the past few years can be collected to obtain diffuse proportion denoted by  $\delta_d$  (Equation 1) and transmissivity denoted by  $\delta_t$  (Equation 2) [66], in which  $P_{clear}$ ,  $P_{partlycloudy}$ , and  $P_{cloudy}$  are the proportions of days that are clear, partly cloudy, and cloudy. Then, the two indices can be used to compute  $u$  based on the Points Solar Radiation toolbox in ArcGIS Pro [67].

$$\delta_d = 0.20P_{clear} + 0.45P_{partlycloud} + 0.70P_{cloudy} \quad (1)$$

$$\delta_t = 0.70P_{clear} + 0.50P_{partlycloud} + 0.30P_{cloudy} \quad (2)$$

## 2.2. Solar-charging scooters at parking stations

This study assumes that scooters will return to the nearest station immediately when they are left outside the stations and their battery level is below a threshold (i.e., 3.75% of the full battery capability). If scooters cannot travel to the nearest station after serving the last trip by utilizing their battery, then they need to be rebalanced by manpower. The electricity generated by a PV module with a size of  $a$  at a station  $i$  for a time period  $t$  will be recorded as  $e(i, a, t)$ . All the scooters parking at the same station will be charged evenly based on the parking time and the current solar PV potential. This study will not optimize charging capacities in different stations, assuming that all the PV modules have the same size allocated on near-ground horizontal surfaces with 20% transition efficiency, which has been widely achieved in the industry. Based on the above architecture, an online system can be developed to investigate the performance of the solar charging potential for shared e-scooters. It is worth noting that some scooters were returned close to the parking stations mainly due to the uncertainty of GPS location [10]. Thus, this study relocates scooters to the nearest station if they are within a 100m radius to allow solar charging.

## 2.3. A battery-aware real-time shareability network

It is imperative to design a real-time shareability network in aware of the battery range to build a scooter-sharing system powered by solar charging. In our designed docking scooter-sharing service, a fleet size defined by the number of operated e-scooters and denoted by  $n$  will be initialized with an even distribution across parking stations, and each scooter has a full battery capacity  $cap$ . Users are required to reserve scooters before the usage with  $(o, d, t_r)$  provided, where  $o$  and  $d$  are the trip origin and destination locations constrained in the set of the stations and  $t_r$  is the reservation time that should be at least with  $t_s$  minutes (such as 5 minutes) ahead of the departure time  $t_o$ . This setting allows the system to optimize the dispatching of scooters to users. If there are no scooters available at the station, users are suggested to walk up to  $d_w$  distance away to get a scooter. In practice,  $d_w \in [50, 100]$  (m) is considered to be a reasonable choice given that scooters mainly serve for short trips. If scooters are still unavailable within a  $d_w$  radius, the system will consider repositioning scooters to maximize the service capability. Since scooters with the autonomous traveling

functionality have been in the driving test phase [52], this study assumes that scooters have a limited autonomy capability to reposition themselves if needed. The stations are associated with the nearest node of the road graph so that scooters arriving at or departing from specific stations can be determined.

In the system, each reservation is recorded as  $r = \{rid, t_o, i_o, i_d, o, d\}$ ,  $\forall r \in \mathcal{R}$ , meaning that a user reserves a scooter with a reservation ID  $rid$  to depart from the station  $i_o$  at time  $t_o$  and arrive at the station  $i_d$ , corresponding to locations  $o$  and  $d$ . To serve the user, a scooter with an ID  $sid$  will consume the battery  $e_t$  for travelling a total trip distance  $d_t$ , and during the service its status is updated instantly for the current location  $c$ , the remaining battery  $e_c$ , and the travelled distance  $d_c$ , so that a scooter is described by  $s = \{sid, rid, c, e_t, e_c, d_t, d_c\}$ ,  $\forall s \in \mathcal{S}$ . Particularly,  $rid = 0$  means that the scooter is standby to provide service and  $rid = -1$  means that the scooter is travelling for the rebalancing purpose. The scooter  $sid$  follows the shortest path  $sp$  from  $o$  to  $d$  to provide service for  $rid$ , which is denoted by  $p = \{rid, sid, o, d, sp\}$ ,  $\forall p \in \mathcal{P}$ .

During each time interval  $t_s$ , the system receives a set of reservations  $R$  and updates the statuses of all the scooters  $\mathcal{S}$  in one of the three categories, i.e., parking regularly at the stations  $O_s$ , parking inappropriately outside stations  $O_o$ , and serving user trips or making repositioning  $O_t$ . Then, the system dispatches scooters  $S_s$  to reservations  $R_s$  with the three conditions: (i) the scooters and the reservations share the same departure locations (either at or outside the parking stations), (ii) the current battery level of a scooter  $s$  can support the user trip following the shortest path from  $o$  to  $d$ , and (iii) the scooter with the highest battery level is assigned to the reservation having the longest trip distance. If there are not enough scooters available or not enough battery level, then all the nearby scooters will be listed as candidates  $S_c$  when their battery level can complete the repositioning trip during the next time interval and can continuously support the trip of each unserved reservation  $r \in R_u$ . In this case, all the reservations are organized as  $R = R_s \cup R_u$ .

Furthermore, the system optimizes the dispatch of the scooters in  $S_c$  to the reservations in  $R_u$  by satisfying two consecutive priorities, i.e., maximizing the number of reservations, and minimizing the total trip distance of all the reservations to save the electricity consumption. The optimization is achieved in two steps. Firstly, if a scooter  $s \in S_c$  can serve a set of

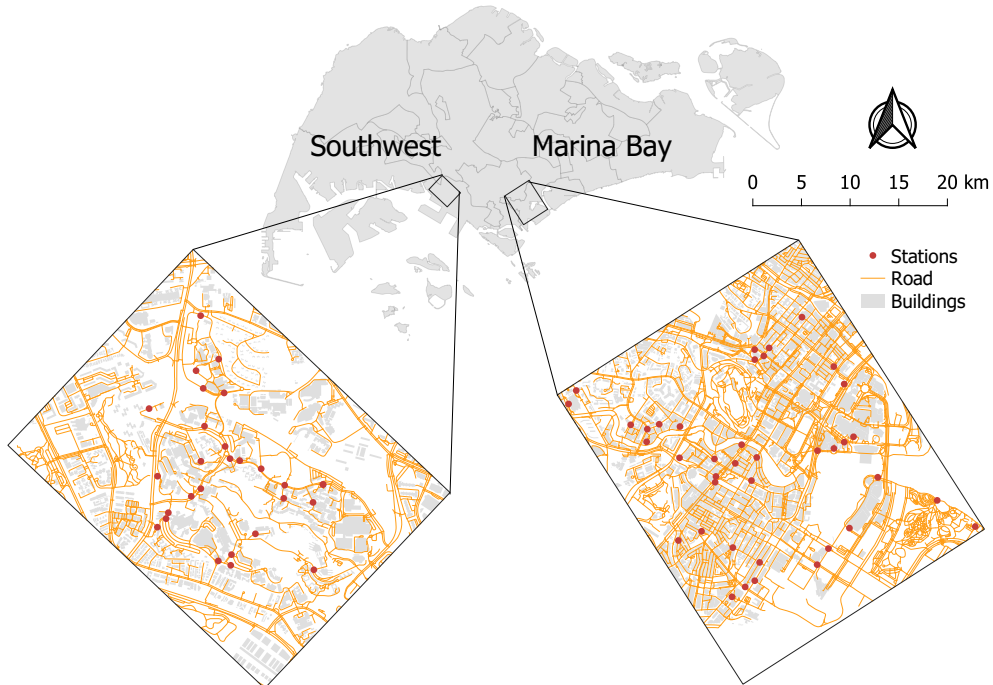


Figure 2: The two study areas of Southwest (SW) and Marina Bay (MB) in Singapore.

the reservations  $\{r_1, \dots, r_n\} \subseteq R_u$  while  $r_1$  can *only* be served by  $s$  and  $\{r_2, \dots, r_n\}$  can be served by other scooters, then  $s$  will be dispatched to  $r_1$  with the highest priority. The system will loop this step until all the reservations in such a scenario are served. Secondly, if  $r \in R_u$  can be served by a set scooters  $\{s_1, \dots, s_n\} \subseteq S_c$  and  $S_c$  can also serve several reservations including  $r$ , and the path from  $s_i$  ( $i = \{1, \dots, n\}$ ) to  $r$  is the shortest, then  $s_i$  will be dispatched to  $r$ . The system will also perform loop computation until all the reservations in this case are served. Some reservations may not be served since there are not be enough scooters available.

### 3. Empirical investigation

#### 3.1. Study area

Singapore emphasizes the development of public transit to mitigate the pressure on increasing traffic demand since it is one of the few cities having the highest density of population across the globe. As an alternative to conventional commuting methods, micro-mobility in Singapore had experienced a rapid transition from the decline of dockless bike-sharing to the expansion of docking scooter-sharing services. Compared with the dockless bike-sharing service that has caused severe chaos in public spaces, docking scooter-sharing service has solved this problem with the implementation of a new regulation that scooters can only travel between a cluster of fixed parking stations in designated areas and users will face a certain penalty if they return scooters inappropriately. However, scooter-charging has be-



come a new challenge as trips driven by charging purposes took around 31% of the total trips in the downtown area in Singapore [10]. In the other perspective, Singapore has abundant solar energy throughout the year as the city-state is located almost on the equator with little cloud cover. Therefore, Singapore is an ideal study area to explore the feasibility of optimizing the operational efficiency of scooter-sharing services through the integration of solar charging and a real-time shareability network.

### 3.2. Data collection and preprocessing

This study collected scooter-sharing dataset from the main service operators in Singapore. The dataset covers the neighborhood of Marina Bay (MB) in downtown, with an area of 3.0 km  $\times$  3.5 km, and Southwest (SW) mainly covering the campus of the National University of Singapore, with an area of 2.0 km  $\times$  2.6 km (Figure 2). Data has been recorded for 28 days in February 2019. Thus, the trips in the two areas are organized as two independent datasets  $\mathcal{R} = \{R_{MB}, R_{SW}\}$  that 348 scooters produced total 11445 total trips with 39 parking stations in MB and 463 scooters made total 40380 total trips with 28 parking stations in SW. It is found that the numbers of user trips, charging trips, and repositioning trips are 4697 (41.04%), 3631 (31.73%), and 3117 (27.23%) in MB, and 34729 (85.06%), 3453 (8.46%), and 2648 (6.48%) in SW. This means that operators make an additional of 58.96% and 14.94% charging and repositioning trips in MB and SW, respectively.

For  $\forall r \in \mathcal{R}$ ,  $r = \{id, o, d, i_o, i_d, e_o, e_d, t_o, t_d\}$ , meaning a trip  $r$  is recorded by a scooter ID  $id$ , departure and arrival GPS locations  $o$  and  $d$ , the corresponding scooter stations  $i_o$  and  $i_d$ , the battery levels in percentage  $e_o$  and  $e_d$ , and the time  $t_o$  and  $t_d$ . Based on the change of battery levels, the trips can be categorized as user trips if  $e_o > e_d$ , repositioning trips if  $e_o = e_d$ , and charging trips if  $e_o < e_d$ . It is important to notice that battery change is reported between 0 and 100%, and this study assumes a full battery capacity at 800 Wh that can support trip distance up to 50 km, which has also been achieved by scooter sharing operators [48, 68].

Since continuous locations during the trips are not reported, we construct a *weighted* and *directed* graph from OpenStreetMap [69] to compute paths of the trips by assuming that all the trips follow the shortest path from  $o$  to  $d$ , which has been suggested being reliable for the trajectory distribution patterns in Singapore [10]. The graph excludes highways but retains



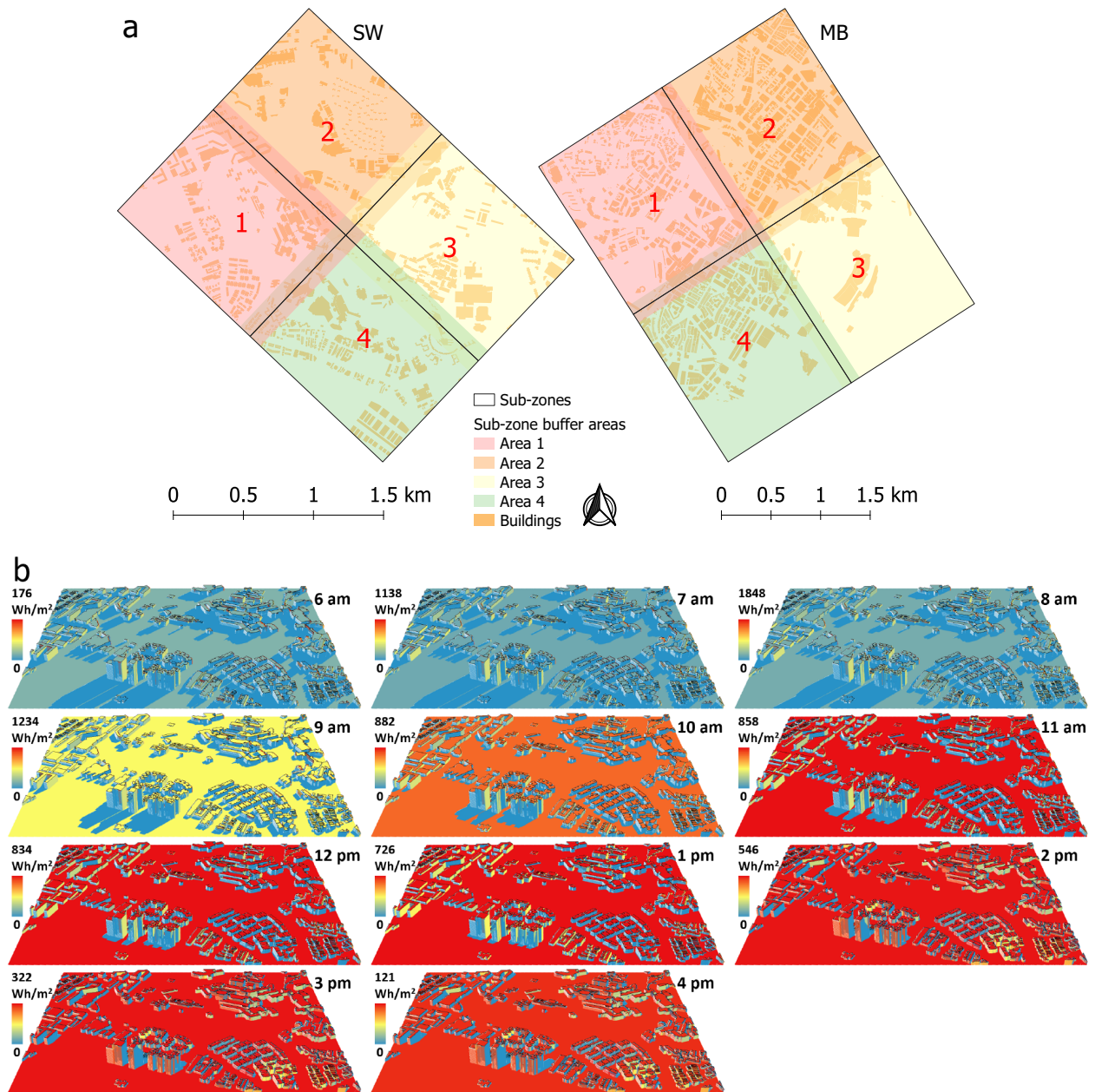


Figure 3: Computation of hourly solar irradiation distribution on 3D urban surfaces in MB and SW. (a) Each study area is divided into four sub-areas. (b) Hourly solar irradiation distribution from 6 am to 4 pm for Area 1 in SW.

sidewalks, bike lanes, and roads. Weights of edges in the graph are equal to the lengths of the respective road segments. This study matches the origins and destinations of the trips and scooter stations to the closest nodes of the graph.

### 3.3. System development

To achieve fast computation of solar PV potential on 3D cities, each study area is divided into four sub-areas that overlap with each other with a constant width so that each sub-area can be computed in parallel and the shadow effect from buildings located in the overlapping area can be considered (Figure 3a). After computation, the four areas without overlapping are merged as a unified study area, resulting in removing the marginal shadow effect. The spatial resolution of the 3D point clouds was 1 m for the empirical investigation, which generated 15.9 million points in MB and 7.2 million points in SW (Figure 3b) to record

---

**Algorithm 1:** SolarCharging(bty\_cap INTEGER, c\_t TIMESTAMP, t DOUBLE PRECISION)

---

```

1 UPDATE scooter AS sco
2 SET bty_cur = bty_cur + e4s.e
3 FROM (SELECT e.sid AS sid, ((e.elec / 60 * t) / s.sco_cnt) AS e
4 FROM hr_elec
5 LEFT JOIN
6 (SELECT staid_o AS sid, COUNT(*) AS sco_cnt
7 FROM scooter
8 WHERE did = 0 AND sid_o>0 GROUP BY sid_o) AS s
9 ON e.hod = EXTRACT(HOUR FROM c_t)
10 WHERE s.sid = e.sid AND s.sco_cnt IS NOT NULL) AS e4s
11 WHERE sco.did = 0 AND sco.sid_o>0 AND sco.sid_o = e4s.sid;
12 UPDATE scooter SET bty_cur = bty_cap WHERE bty_cur > bty_cap;

```

---



---

**Algorithm 2:** DispatchSco2DmdFromStation(c\_t TIMESTAMP, t DOUBLE PRECISION)

---

```

1 CREATE TABLE dmd_cur AS
2 SELECT id AS did, sid_o, sid_d, source, target, loc_o, loc_d, bty_need,
3 ROW_NUM() OVER (PARTITION BY sid_o ORDER BY sid_o) AS rn
4 FROM demand AS dmd
5 WHERE dmd.t_o>=c_t AND dmd.t_o<c_t + t * 60 * '1 second'::INTERVAL
6 ORDER BY sid_o, rn;

7 CREATE TABLE sco AS
8 SELECT *, ROW_NUM() OVER (PARTITION BY sid_o ORDER BY sid_o) AS rn
9 FROM scooter
10 WHERE did=0 AND sid_o>0;
11 ORDER BY sid_o, rn;

12 CREATE TABLE demand_cur_match AS
13 SELECT DISTINCT dmd.*, sco1.sco_id, sco2.bty_cur
14 FROM demand_cur AS dmd
15 LEFT JOIN sco AS sco1
16 ON dmd.loc_o = sco1.loc_c
17 AND dmd.rn = sco1.rn
18 LEFT JOIN sco AS sco2
19 ON dmd.loc_o = sco2.loc_c
20 AND dmd.bty_need <= sco2.bty_cur;
21 ORDER BY sid_o, rn;

```

---

heterogeneous solar potential. The number of point clouds is almost double in MB than that in SW because MB is in the downtown area and has a large number of skyscrapers, leading to a large area of urban surfaces. Hourly cloud-cover data in February between the years 2015 and 2017 have been collected from World Weather [71] to estimate direct and diffuse solar irradiation.

The model was implemented as a set of hierarchical SQL functions, which were incorporated into an iterative computational framework in a spatial database management system of PostgreSQL 11 [70]. Algorithm 1 introduces the solar charging process for scooters parking at the stations. Specifically, Lines 6-8 summarize the number of scooters (sco\_cnt) currently parking at each station (with station ID sid>0) as the scooter-demand ID is zero (did=0).

Lines 3-10 determine the amount of electricity ( $e$ ) that each scooter can be charged at a station for a period of  $t$  minutes, based on the hourly PV electricity generation record ( $hr\_elec$ ) obtained from the 3D solar estimation model. Lines 1-11 update the electricity level of each scooter after the solar charging. Line 12 ensures that the current electricity level is no larger than the full battery capacity. Algorithm 2 demonstrates a simple case that scooters parking at the stations are dispatched to the users without the requirement of repositioning. Particularly, Lines 1-6 list the mobility demand that will depart from a station ( $sid_o$ ) and arrive at the other station ( $sid_d$ ) in the group of each charging station ( $sid_o$ ) during an iterative period, which will be used for the dispatching optimization. Lines 7-11 list a set of scooters having not been reserved in the group of each solar charging station. Then, Lines 15-17 ensure that scooters will depart from the current parking station, and Lines 18-20 ensures that the current battery level can successfully support the electricity demand of the reserved trips. Finally, Lines 12-21 list the scooters that will be dispatched to the new demands, which can be used to update the real-time status of the scooters.

## 4. Analysis of the spatio-temporal battery demand

### 4.1. Statistics of the fleet size and battery usage

Before performing a real-time simulation of the designed shareability network, the dataset allows us to estimate the solar charging potential for all the scooters operated in the real world, which can provide a better understanding of the proposed solar charging solution through comparison. Since usages of all scooters are recorded in the dataset, the fleet size defined by the number of the operated e-scooters can be determined, and the amount of charging can be estimated for each scooter during the simulation period. This allows a simple estimation of the potential of solar charging to support scooter-sharing operations, without a need for autonomous functionality.

First of all, this study presents statistics about the fleet size and battery usage of the scooters. Figure 4a shows the daily battery usage (i.e., the percentage of the full battery capacity) in the x-axis and the corresponding usage frequency of all the scooters in the y-axis, which is obtained by summing up the decrease of the battery level between 0-100% when reserved trips were completed. Overall, less than half of the battery capacity is used

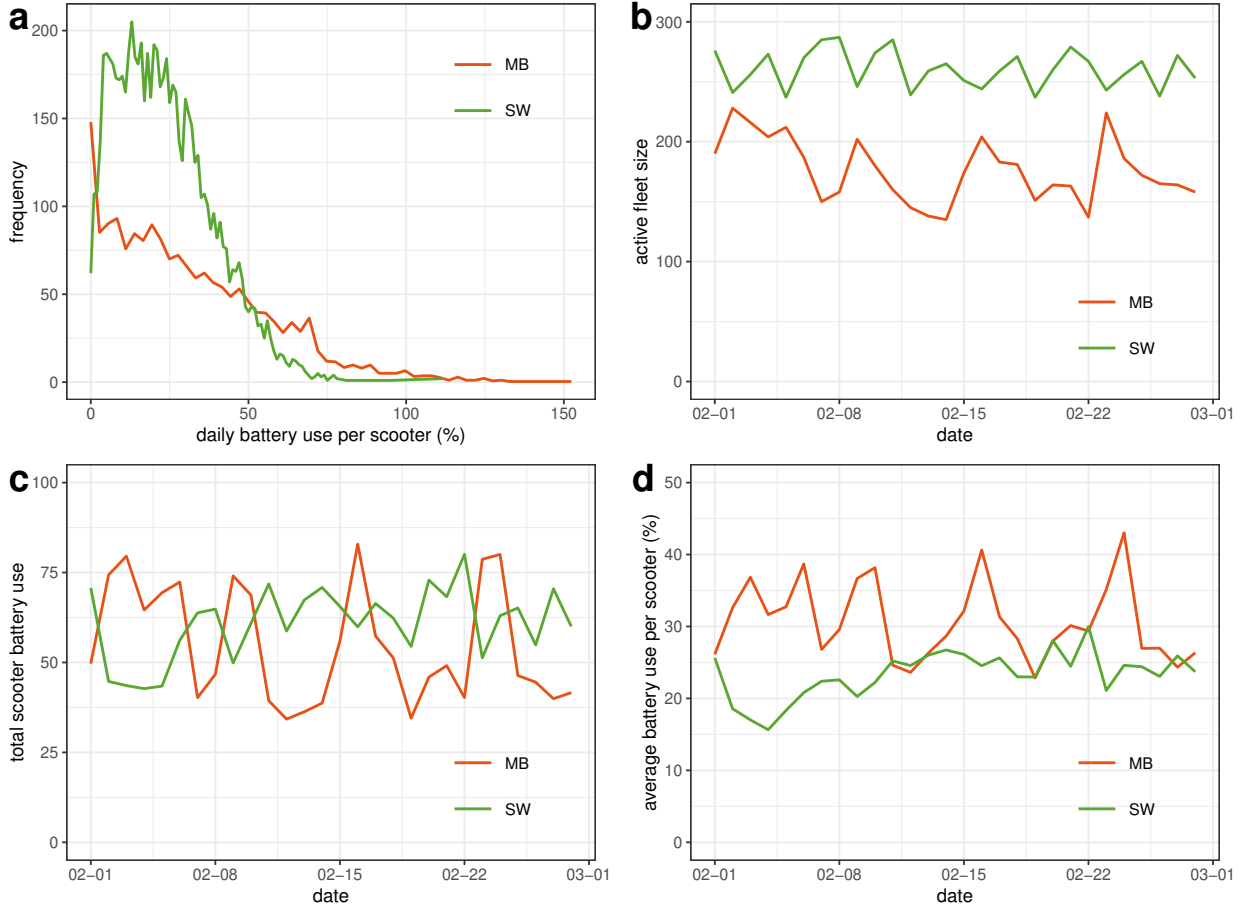


Figure 4: The statistics of battery usage for scooters. (a) Distribution of battery usage per scooter per day. (b) Active fleet size of the scooters. (c) Total battery usage of all the scooters subject to the full battery capacity of one scooter. (d) Average battery usage per scooter per day.

on one day in most cases. While, there are a few scooters that used more than the full battery capacity, which means that these scooters were charged on that day. The active fleet sizes, defined by the number of scooters making at least one trip each day, are between 150 and 200 in MB and between 250 and 300 in SW (Figure 4b). Following this situation, the total electricity consumption is about 50 to 75 times the full battery capacity of one scooter (Figure 4c), and the average battery usage per scooter per day, defined by the percentage of the full battery capacity, is approximately between 20% and 40% of the battery capacity (Figure 4d). It is found that most scooters consumed less than 100% or even 50% of the full battery capacity.

#### 4.2. Relationship between battery usage and trip distance and duration

To better estimate the electricity consumption, this study analyzed trip distance and trip duration as a function of battery usage (Figure 5), which was limited to trips shorter than two hours. When considering trip distances, a correlation can be established for short trips that are below 20% battery use with an approximate distance of 2 km (Figures 5a, 5b). The best linear fit for MB is  $d = 60.17 \times b + 715.55$  (Figure 5a), where  $d$  is the estimated trip

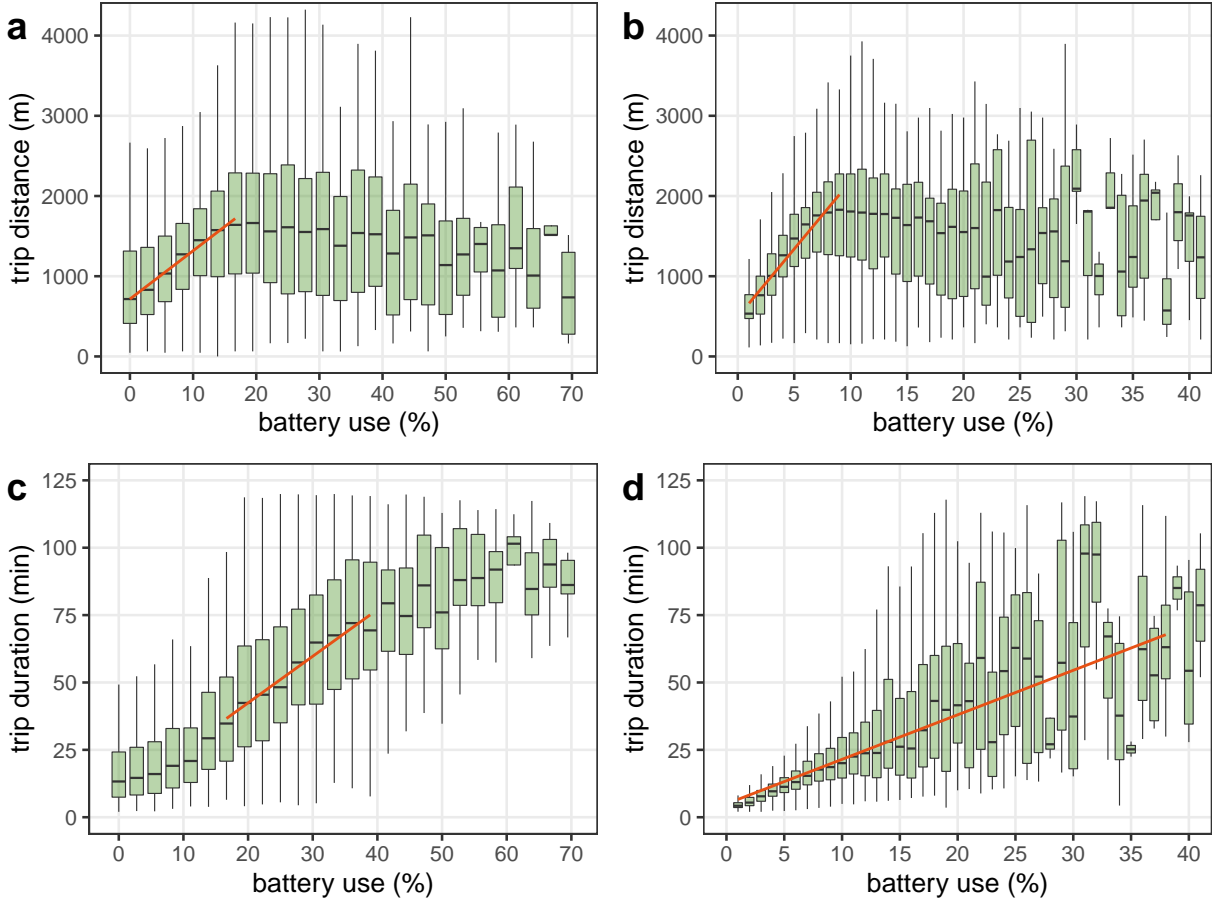


Figure 5: Trip distance and duration subject to battery usage. The blue lines are linear fits to the median values in regions with significant linear trend. (a) Trip distances as a function of battery usage of scooters in MB. (b) Trip distances as a function of scooters’ battery usage in SW. (c) Trip duration as a function of battery usage of scooters in MB. (d) Trip duration as a function of battery usage of scooters in SW.

distance (m) and  $b$  is the used battery level (%) during the trip, and the best fit for the SW is  $d = 169.4 \times b + 492.8$  (Figure 5b). For trips that consumed more electricity, the total distance shows large variations without a clear trend. This can be explained that the short trips with limited battery usage are point-to-point journeys so that the estimated path is an appropriate approximation. On the other hand, there are longer trips that the scooters were used either for sightseeing by tourists or for making deliveries by “gig economy” workers of multiple services that offer short notice delivery for food and other goods (e.g., Grab, and FoodPanda), which has been suggested by a case study in Singapore [10]. In these cases, users will make a long journey so that the shortest path between the departure and arrival locations is irrelevant. To account for this effect, this study analyzed the relationship between battery usage and duration of a trip and observed a more reliable trend relating longer trips to larger battery use (Figures 5c, 5d). The best linear fit to the median values is  $t = 1.73 \times b + 7.82$  for MB (Figure 5c), where  $t$  is the trip duration (min) and  $b$  is the used battery level (%) for the trip, and the best fit for SW is  $t = 1.652 \times b + 4.96$  (Figure 5d).

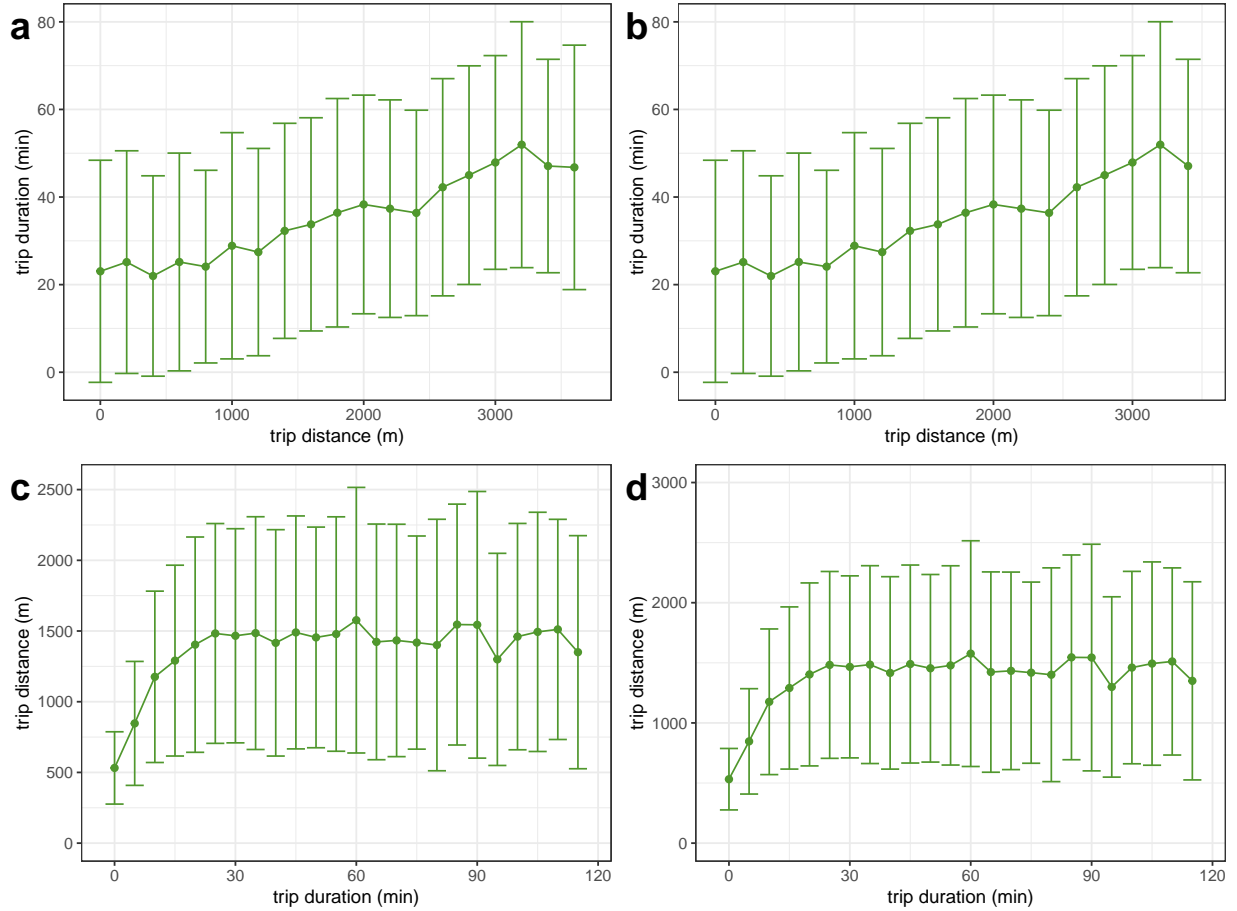


Figure 6: Relationship between trip distance and duration. (a,b) Average trip duration as a function of estimated distance in MB and SW (grouped in 200 m distance intervals), respectively. (c,d) Average trip distances as a function of trip duration in MB and SW (grouped in 5 min time intervals), respectively.

#### 4.3. Relationship between trip distance and duration

Furthermore, this study explores the relationship between estimated trip distance and trip duration. The analysis shows a weak trend when grouping trips by distance (Figures 6a, 6b), i.e., trips with longer estimated distance tend to take a longer time. However, the duration of the long-distance trips has a large variation as well, consistent with the fact that there are a significant number of trips with short estimated distance but long time duration. When grouping trips by duration (Figures 6c, 6d), a relationship can be established with estimated distance for short trips that are approximately shorter than 25 min and 1.5 km on average. For longer trips, the estimated distances are not dependent on the trip duration, meaning that these are not point-to-point trips.

#### 4.4. Hourly averaged total battery use

It is also important to reveal the temporal distribution of the total battery usage since solar power is an intermittent source so solar charging is unavailable after sunset. Figure 7 presents hourly averaged battery usage of all the scooters, displayed as an index subject to the full battery capacity of one scooter. The figure shows two opposite trends that major usage in MB occurs in the evening and night versus major usage in SW happens in the



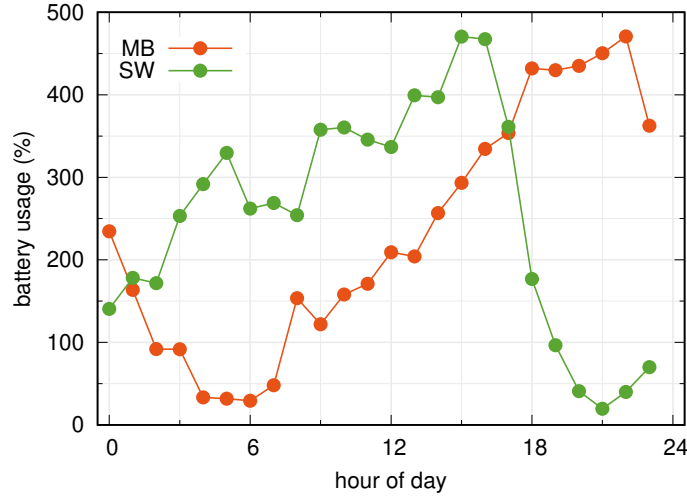


Figure 7: Hourly averaged battery usage of all the scooters subject to the battery capacity of one scooter.

early morning and afternoon. The two trends are reasonable because MB has many world-famous tourist attractions that visitors usually make a trip after the sunset to avoid the exposure of big sunshine during the daytime, while a university campus is located in SW that scooters mainly serve for the commuting of colleague students. This observation also has two implications. For scooters in MB, most of them can be charged during the daytime, and the battery capacity should be large enough so that charging during the day can provide a sufficient travel range after sunset. As the daily battery usage of most scooters does not exceed 100% (Figure 4a), fully charging them during the daytime may provide enough energy for evening usage. For scooters in SW, high battery usage during the daytime indicates frequent use of scooters that might hinder solar charging. Nevertheless, scooters should still be able to get a reasonable amount of solar charging since scooters were parking at stations most of the time with a trip duration shorter than one hour every day (Figure 6b). Based on this evidence, battery storage will not be considered in the real-time estimation of solar charging potential.

## 5. Estimation of solar charging potential based on real trip data

According to one study on three-dimensional solar cities [24], the daily average solar irradiation throughout the year is  $5532 \text{ Wh/m}^2/\text{day}$  in Singapore, which considered three-years historical weather between 2016 and 2018. PV modules used in this study are expected to have a 20% transition efficiency of solar irradiation that corresponds to an average energy generating capacity of  $1106.4 \text{ Wh/day/m}^2$ . This means that the total energy demand could be satisfied with a total of  $45.19 - 67.79 \text{ m}^2$  of PV modules in theory. Note that this would

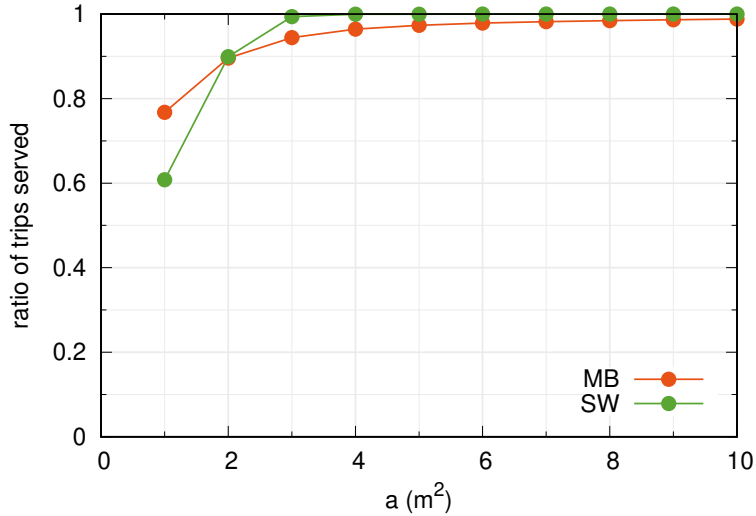


Figure 8: The ratio of successful trips in the y-axis as a function of the PV size denoted by  $a$  in the x-axis at each station.

require ideal charging during daylight hours since charging will be constrained by the availability of scooters. In this section, estimating solar charging potential is based on the total scooters and their served trips as recorded in the dataset. For each trip, battery usage is expressed in percentage of the full battery capacity, and scooters get solar charging when parking at the stations, as proposed in Section 2.2.

### 5.1. Estimation based on all trips

In a simple case, this study assumes all trips happening as recorded in the dataset regardless of whether they were user-demand trips or repositioning trips, or whether the remaining battery level can complete the trips. Then, the battery level decreases during the trips according to the original dataset, and the battery level increases through solar charging when the scooters are parking at stations. Over the course of the simulation, the number of successful and unsuccessful trips are counted. Specifically, a trip is successful if the scooter has enough battery level to complete the trip, while a trip is unsuccessful if the battery level is not enough. This study assumes that unsuccessful trips will be served by instant manual charging to relocate scooters to new destinations. With the assumption of 800 Wh battery capacity, the result of this simulation is the ratio of successful trips subject to the size of PV modules installed at each station. In this case, it is found that more than 95% of the real trips can be served in both MB and SW if each station is equipped with PV modules at a size of 3 m² (Figure 8).



### 5.2. Estimation based on variable trips

Furthermore, this study carries out a more complex estimation that trips can only happen when a scooter has sufficient battery level. Otherwise, the trip will not be served and thus the scooter will not move. This implies that over the course of the simulation, the distribution of scooters will diverge from that in the original dataset, since some trips are omitted as they cannot be served due to the low battery level. This might lead to further trips not being served because the scooter is no longer at the start location of the next trip. In contrast to the previous case, this study does not require the same scooter to serve the trip as in the original dataset, but allows any scooter to be assigned to a trip that is within a search radius of  $r_{\max}$  of the original departure location and has sufficient battery level. This can result in a better performance than an original scooter with an insufficient battery level can be replaced by another one with a sufficient battery level to serve the trips.

As a result, Figure 9 shows that the ratio of successfully served trips is increasing with the increase of  $r_{\max}$  from 100 to 300 meters, which is understandable since more scooters will be available with enough battery level to serve the same trip with the increase of  $r_{\max}$ . Also, it is noticed that scooters cannot get solar charging if they are used continuously, which is a real situation revealed from the dataset. In this case, a substitute needs to be found, which depends on the actual distribution of scooters and the designated search radius. The other important factor is whether rebalancing of the scooters is performed by the operators to meet the real-time mobility demand from users. In this consideration, this study compares two different scenarios that certain trips are omitted due to the unavailability of the scooters or these trips are served through rebalancing scooters (Figure 9). It is found that the serving ratio without rebalancing is significantly lower in MB (Figure 9a) than that in SW (Figure 9b), where the spatio-temporal demands of trips in MB are more unpredictable. This is because a significant amount of the trips in MB are likely performed by tourists who do not return the scooters to the parking stations; instead, they abandoned scooters and accepted certain penalty to be charged by the operators [10]. Another observation from Figure 9 is that rebalancing is fundamental to maximize the possibility of solar charging. Without rebalancing, the amount of the served trips is independent of the size of the PV modules; with rebalancing, the amount of the served trips can reach up to a saturation level

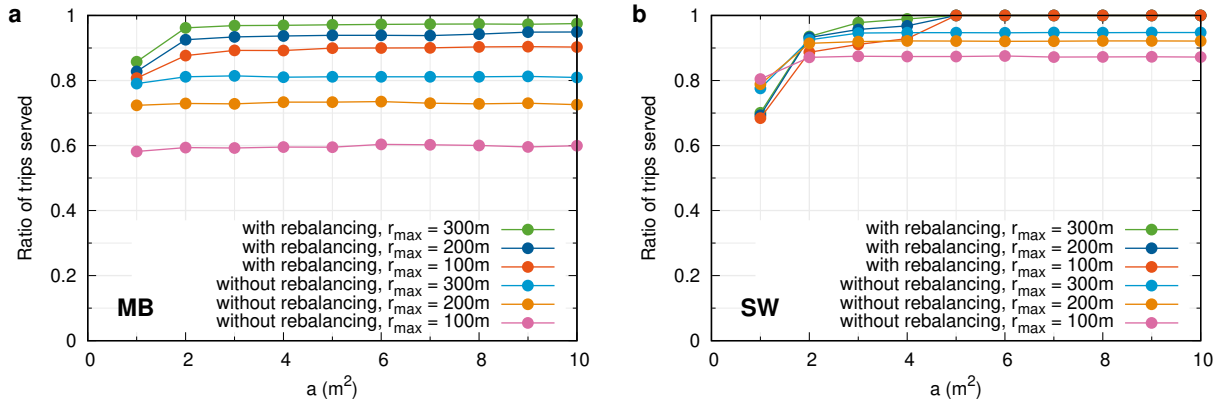


Figure 9: The ratio of served trips in the y-axis as a function of the PV size denoted by  $a$  in the x-axis at each station.

with PV size ranging between 2 to 5  $\text{m}^2$ .

## 6. Real-time estimation of solar charging potential

In reality, a scooter can only be charged when it is parking at a charging station. In this section, the availability of autonomous scooters with a varying fleet size is considered to evaluate the performance of a real system on solar charging of shared electric scooters, based on the real-time shareability network proposed in Section 2.3.

### 6.1. Shareability influenced by the fleet size

As a forthcoming situation, scooters can autonomously reposition themselves so that all manpower costs associated with the scooter rebalancing and charging could be avoided. This motivates us to investigate the performance of the scooter-sharing services when a real-time shareability network is adapted to solar charging platforms. The network obtains the maximum dispatching of available scooters to trip reservations and the minimum total distance of all trips for each iterative period. The optimal configurations of the services are explored through a simulation over 28 days in February 2019, and this study assumes the electricity usage rate of a scooter is 16 Wh/km that has been achieved by scooter manufacturers [48, 68].

Since more scooters mean higher operational costs for operators, a balance between a small fleet size and a high service rate is preferred. This study firstly explores the minimum fleet size by assuming that each scooter starts from 100 Wh with a full battery capacity at 800 Wh and a constant speed at 15 km/h, the scooter reservation time is 5 minutes, and the PV module at each scooter station is 12  $\text{m}^2$ . Since MB has 39 and SW has 28 parking stations, the fleet sizes of scooters will be  $\{78, \dots, 468\}$  and  $\{56, \dots, 336\}$  in the two areas respectively if

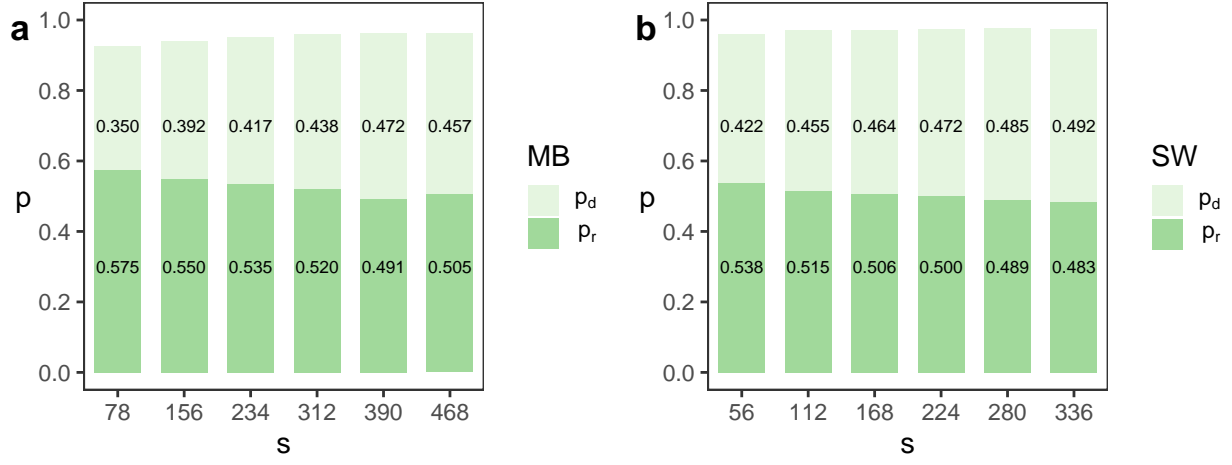


**Figure 10:** The rate of successfully served trips ( $p$ ) changes with the varying of the fleet size ( $s$ ) of the scooters. (a) The study area in MB. (b) The study area in SW. The  $p$  values presented by the blue bars is decomposed by  $p_d$  that does not need repositioning and  $p_r$  that needs repositioning.

each station initializes a number of scooters equaling to  $n = \{2, 4, 6, 8, 10, 12\}$ . It shows that the rate of successfully served trips ( $p$ ) has already obtained a value higher than 0.9 when each station starts with two scooters, and  $p$  grows slightly with the increase of  $s$  (Figure 10). The successful serving rate contains two scenarios, corresponding to the situation where scooters are directly available at the charging stations ( $p_d$ ) or need repositioning to the stations ( $p_r$ ). The results demonstrate that  $p_d$  increases versus  $p_r$  decreases in both study areas when  $s$  increases. This is because a larger fleet size allows more scooters available to serve the trips directly at the stations so that repositioning could be reduced. This study considers that 234 scooters in MB and 112 scooters in SW are appropriate to provide adequate services as the rates have been larger than 0.95 and 0.97, respectively. In this case, the solar charging solution only needs 24%-67% of the total scooters as there are 348 scooters in MB and 463 scooters in SW in the real world.

## 6.2. Shareability influenced by the reservation time

On-demand mobility provides instant services for users at their designated departure time. However, if scooters are unavailable at the request location and users do not want to involve in any waiting-caused delay, then a reservation is needed to allow on-demand service. In this case, scooters can take the reservation time to make autonomous reposition to meet users. Based on the suggested fleet sizes (i.e., 234 scooters in MB and 112 scooters in SW), minimizing the reservation time is preferred to provide on-demand mobility and enable proper user experience. It is found that  $p$  has a significant growth when the reservation time  $t$  increases from 1 to 5 minutes in both MB and SW (Figure 11). Then,  $p$  grows slowly from

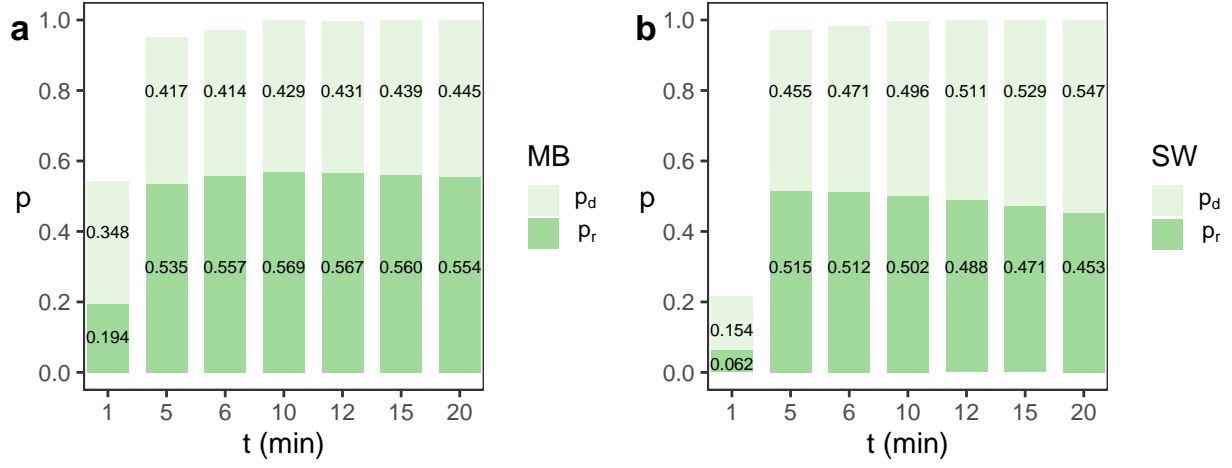


**Figure 11:** The rate of successfully served trips ( $p$ ) changes with the varying of the minimum reservation time ( $t$ ). (a) The study area in MB. (b) The study area in SW. The  $p$  values presented by the blue bars is decomposed by  $p_d$  that does not need repositioning and  $p_r$  that needs repositioning.

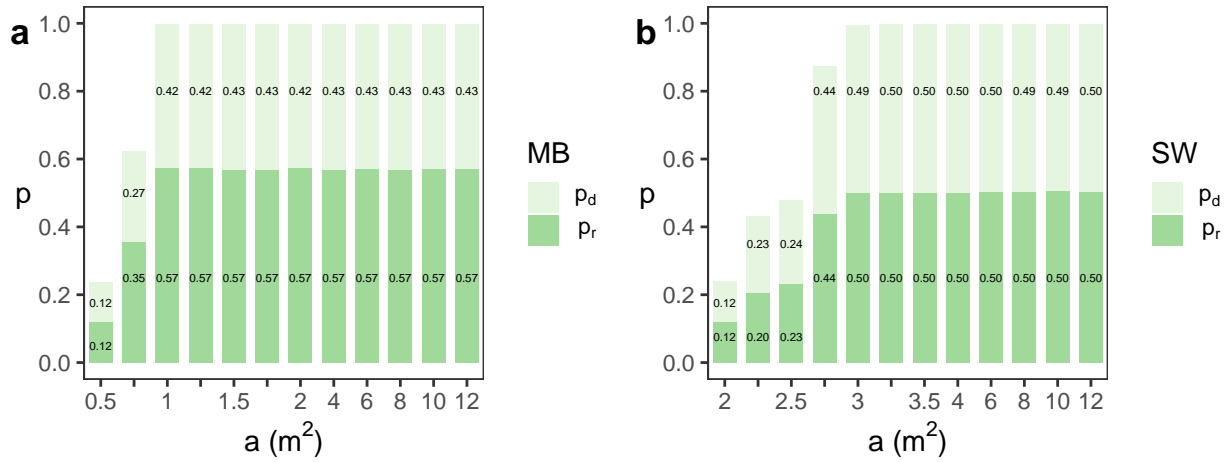


**Figure 12:** The rate of successfully served trips ( $p$ ) changes with the varying of the size of PV modules at each station ( $a$ ). (a) The study area in MB. (b) The study area in SW. The  $p$  values presented by the blue bars is decomposed by  $p_d$  that does not need repositioning and  $p_r$  that needs repositioning.

5 to 20 minutes, and it is larger than 0.99 when  $t$  is 10 minutes. Notably,  $p_d$  grows up while  $p_r$  drops off with the increase of  $t$ . The reason is that the majority of trips will complete when approaching 10 minutes so that more scooters can have a seamless connection at the charging stations to serve the next trip with less need of repositioning. Thus, reservation time at 10 minutes is recommended since it is the shortest time that serves almost all the trips.

### 6.3. Shareability influenced by the PV module size

Considering the limited stations in urban areas and the saving of operational cost, the management of the PV module size is also vital to establish an efficient solar charging solution. Based on the determined fleet sizes (234 in MB and 112 in SW) and reservation time (10 minutes) with an initial battery of each scooter at 100 Wh, each station needs PV modules at 1.00 m² in MB and 3.25 m² in SW to serve 99.7% of all the *real* trips (Figure 12). This means that the total PV size for all stations is 39 m² for MB and 91 m² for SW. The

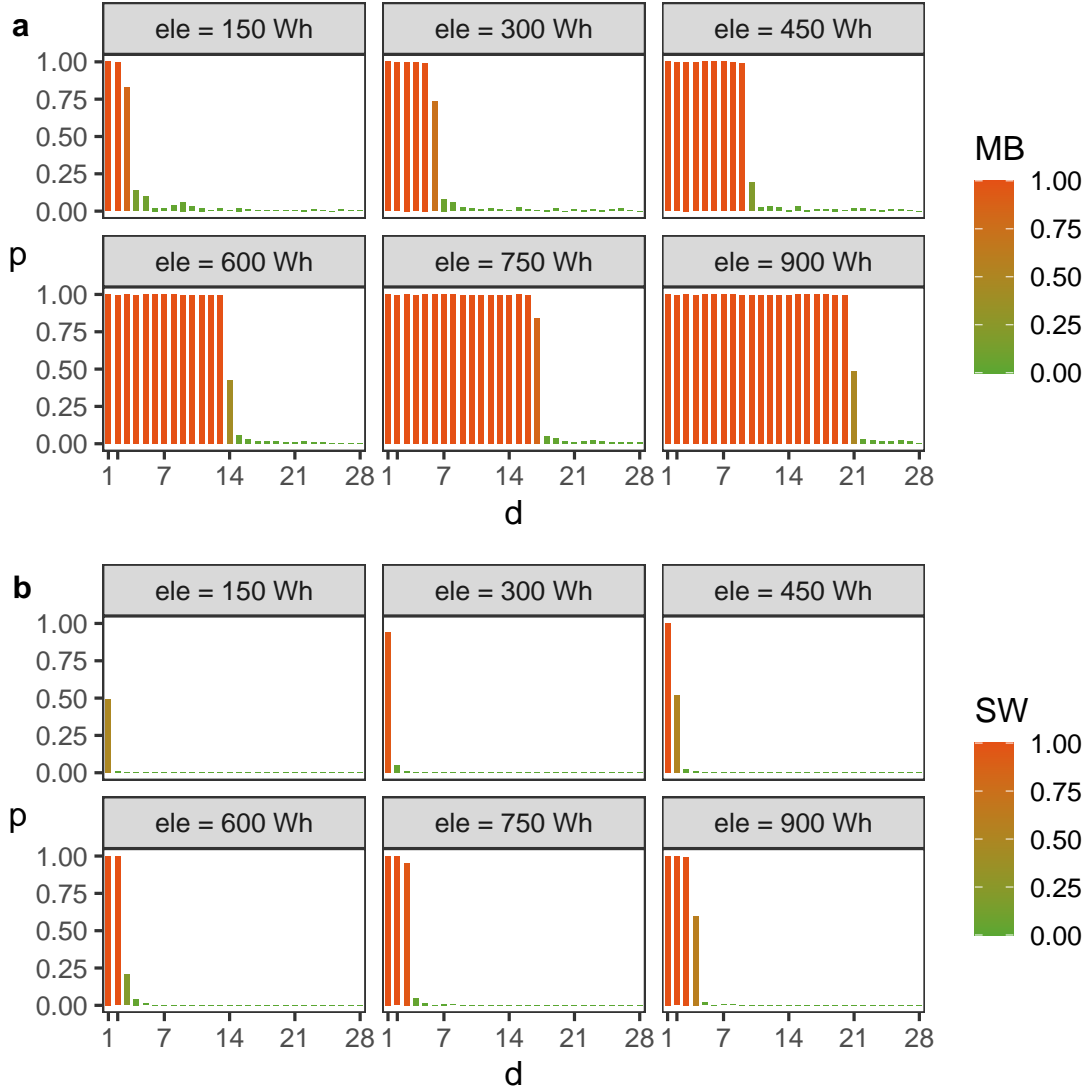


**Figure 13:** The rate of successfully served trips ( $p$ ) over 28 days, by assuming that each scooter starts from the same full-battery level (from 150 Wh to 900 Wh) in each independent experiment and there is no solar charging due to continuous of thick clouds. (a) The study area of MB. (b) The study area of SW.

result obtains a linear regression roughly between the size of the PV modules and the number of all the trips, i.e., 11,445 trips in MB and 40,830 trips in SW, indicating the effectiveness of the real-time simulation. Different from the two simulations in Sections 6.1 and 6.2,  $p_d$  and  $p_r$  in each study area maintain a constant ratio when  $p \approx 1$ , disregarding the size of PV modules. This means that scooters can get solar charging with equal opportunities when arriving at the stations during the daytime, which will not affect the spatial distribution of scooters. Particularly,  $p_r \approx 0.6$  in MB and  $p_r \approx 0.5$  in SW when  $p \approx 1$ . This suggests that scooters in MB need more frequent repositioning to serve on-demand mobility even though they have a larger fleet size, which indicates a diversity of origins and destinations in MB.

#### 6.4. Resilience of the scooter-sharing service

A major concern of the solar charging solution is the resilience of the service when confronting continuous cloudy days that PV modules can only receive limited solar irradiation. To investigate the resilience when confronting unfavourable weather, this study assumes an

extreme condition that there is no solar irradiation at any time of the day and initializes each scooter from the full battery capacity at  $ele$ , where  $ele$  increases from 150 Wh to 900 Wh gradually in each independent experiment over the four weeks. It shows that, with the increase of the full battery capacity, the sharing service can support almost all the trips with  $p \approx 1$  in the y-axis for 2 to 20 days in the x-axis in MB (Figure 13a) and 0 to 3 days in SW (Figure 13b). The extreme test suggests that the proposed solar charging solution can achieve a self-supporting service for 3 to 20 days without any additional charging because a scooter with a full battery capacity between 750 and 900 Wh has already been implemented widely by industry, and the assumed extreme weather is unlikely happening in Singapore even during the raining season. In comparison, scooters in MB can provide services much longer than SW when  $ele = 900$  Wh. The reason is that MB and SW have 234 and 112 scooters respectively, which means that the PV electricity generation in MB is approximately twice larger than SW, while MB has only one-fourth of the total demands of SW.

## 7. Discussion and conclusion

This study integrates solar charging stations, real-time shareability networks, and autonomous functionality to tackle the problem that shared e-scooters with a limited battery capacity need intensive charging trips, which implies significant manpower cost and impedes the availability of the scooter-sharing service. The hourly PV charging is estimated by considering the direct and diffuse solar irradiation and the shadow effect from nearby buildings. Based on the optimized configurations on the PV size, the fleet size, and reservation time, the system only needs 2.75% and 2.06% of the original charging trips and 1.00 m<sup>2</sup> and 3.25 m<sup>2</sup> of the PV modules in MB and SW, respectively, to serve nearly 100% of the real trips made by users.

If charging one scooter costs \$8 comparable to Lime paying between \$3 to \$20 [14], then it will save more than \$56,000 in the four weeks according to the total number of the charging trips, which can accumulate to \$672,000 throughout a year with the same charging intensity. The saving will even be more significant if the service expands to the whole city since they are operated in a very limited area currently in Singapore. On the other hand, considering the current PV module is \$100~\$150 per square meter with 20% transition efficiency and

200 W/m<sup>2</sup> rated power in the worldwide market and the total needed PV size is 130 m<sup>2</sup> in the two study areas, the cost of making such solar charging platforms will be \$19,500 approximately. If the life-cycle maintenance cost is \$0.72 per watt and a labour cost is \$30.15 per hour [72], then the total maintenance cost will be \$18,720 and the monthly manpower cost will be \$7236 (8 working hours per day and 30 working days per month). Besides, it only needs \$100 to \$300 extra cost to manufacture an autonomous scooter compared with a regular one [73], which results in a much smaller fleet size needed that can also achieve savings in manufacturing scooters. The above discussion suggests that solar charging can be significantly economical compared to the conventional solution. For scooter sharing services that have been operated in many other cities covering the whole urban area, the proposed solar charging approach may solve the “*electric scooter charging is a cutthroat business*” problem [14].

This study proves that PV charging is a feasible solution for scooter-sharing in a topical city full of abundant solar energy. It is important to notice that the latitude of the city is not the conclusive factor of determining annual solar potential while urban morphology can influence it significantly [24]. To promote such a solution in global cities, the PV charging capability can be improved in several aspects. For instance, charging stations can be placed at locations having demand hotspots, the size and the inclination angle of the PV modules in each station can be optimized to maximize solar harvesting, and battery storage can be integrated to eliminate the mismatch between the energy demand and supply.

Although there are high demands in SW during the daytime, the time when scooters serve shared mobility is not significant long in both study areas, which means that they can get enough solar charging when parking at the stations. Meanwhile, there is little evidence to show that the designed shareability network cannot serve the reserved trips because of the limited battery levels. Therefore, it is reasonable not to build a portable storage unit, resulting in further saving of the operational cost. However, battery storage may be considered in other cities when there is a severe mismatch between instant solar charging and real-time mobility demands.

Real-time simulation shows that the autonomous functionality helps to provide around 50% of all the on-demand mobility. The major reason is that the simulation minimizes the

fleet size of scooters so that frequent repositioning is needed to meet user demands in the next iterative reservation time. Based on the managed fleet size, it does not mean that, without the autonomy, the rate of successfully served trips will have a corresponding reduction. It is because the complete set of on-demand mobility requests has two complementary subsets. One subset contains all the successfully served trips recorded by operators, and the other one corresponds to unsuccessfully served trips and unrecorded in the dataset. For the recorded subset used in this study, some trips will be rejected without autonomy so that more scooters will be available to serve more trips at the request locations at a later time, which does not need autonomous repositioning. For the complete dataset, real-time simulation without autonomy may also allow scooters to serve previously rejected trips. However, this study cannot make a direct comparison since the whole dataset cannot be quantified. Thus, autonomous functionality maximizes the sharing capacity and explores the PV electricity generation capacity based on the currently available dataset.

To summarize, it is crucial to promote solar energy to develop sustainable and liveable cities. Building a large area of solar PV plants in a remote region is not the only way to use solar energy; distributed PV systems installed at solar accumulative areas in cities can also be an effective solution even though these areas may be small and dispersive. This study suggests that we should not judge the impacts of solar energy or other types of renewable energy only based on the generated electricity with zero-emission and zero-cost. It can even create more profoundly social and economic impacts because of the way we use it.

## Acknowledgements

The authors thank the funding support from (i) the National Research Foundation, Prime Minister's Office, Singapore under its Campus for Research Excellence and Technological Enterprise (CREATE) programme, (ii) the Strategic Hiring Scheme (Grant No. P0036221) at the Hong Kong Polytechnic University, and (iii) the General Research Fund (Grant No. 15602619).

## References

- [1] Kan Z, Wong MS, Zhu R. Understanding space-time patterns of vehicular emission flows in urban areas using geospatial technique. *Computers, Environment and Urban Systems*



- 2020;79:101399.
- [2] Zhu R, Wong MS, Guilbert E, Chan PW. Understanding heat patterns produced by vehicular flows in urban areas. *Scientific Reports* 2017;7:16309.
  - [3] Martin E, Shaheen S, Lidicker J. Impact of Carsharing on Household Vehicle Holdings. *Transportation Research Record: Journal of the Transportation Research Board* 2020;2143:150–158.
  - [4] Jin ST, Kong H, Wu R, Sui DZ. Ridesourcing, the sharing economy, and the future of cities. *Cities* 2018; 76:96–104.
  - [5] Shen J, Liu X, Chen M. Discovering spatial and temporal patterns from taxi-based Floating Car Data: a case study from Nanjing. *GIScience & Remote Sensing* 2017; 54(5):617–638.
  - [6] Santi P, Resta G, Szell M, Sobolevsky S, Strogatz SH, Ratti C. Quantifying the benefits of vehicle pooling with shareability networks. *PNAS* 2014; 111:13290–13294.
  - [7] Alonso-Mora J, Samaranayake S, Wallar A, Frazzoli E, Rus D. On-demand high-capacity ride-sharing via dynamic trip-vehicle assignment. *PNAS* 2017; 114:462–467.
  - [8] Hosseinzadeh A, Algomaiah M, Kluger R, Li Z. Spatial analysis of shared e-scooter trips. *Journal of Transport Geography* 2021;92:103016.
  - [9] Hardt C, Bogenberger K. Usage of e-Scooters in Urban Environments. *Transportation Research Procedia* 2019;37:155–162.
  - [10] Zhu R, Zhang X, Kondor D, Santi P, Ratti C. Understanding spatio-temporal heterogeneity of bike-share and scooter-share mobility. *Computers, Environment and Urban Systems* 2020;81:101483.
  - [11] Osorio J, Lei C, Ouyang Y. Optimal rebalancing and on-board charging of shared electric scooters. *Transportation Research Part B* 2021; 147:197–219.
  - [12] Helling B. Get Paid as a Lime Scooter Charger to Pick Up Limes, <https://www.ridester.com/lime-charger/>; 2021 (accessed 12 December 2021).

- [13] Helling B. The Comprehensive Guide to Bird Scooter Charging, <https://www.ridester.com/bird-scooter-charger/>; 2021 (accessed 12 December 2021).
- [14] Hawkins AJ. Electric scooter charging is a cutthroat business, and Lime wants to fix that, <https://www.theverge.com/2019/3/15/18267128/lime-electric-scooter-charging-juicers-harvesting-business>; 2019 (accessed 12 December 2021).
- [15] Chandra Mouli GR, Bauer P, Zeman M. System design for a solar powered electric vehicle charging station for workplaces. *Applied Energy* 2016;168:434–443.
- [16] Fretzen U, Ansarin M, Brandt T. Temporal city-scale matching of solar photovoltaic generation and electric vehicle charging. *Applied Energy* 2021;282:116160.
- [17] Buonomanoa A, Calisea F, Cappielloa FL, Palombo A, Vicidomini M. Dynamic analysis of the integration of electric vehicles in efficient buildings fed by renewables. *Applied Energy* 2019;245:31–50.
- [18] Dorokhova M, Martinson Y, Ballif C, Wyrsh N. Deep reinforcement learning control of electric vehicle charging in the presence of photovoltaic generation. *Applied Energy* 2021;301:117504.
- [19] Guo M, Mu Y, Jia H, Deng Y, Xu X, Yu X. Electric/thermal hybrid energy storage planning for park-level integrated energy systems with second-life battery utilization. *Advances in Applied Energy* 2021;4:100064.
- [20] Schleifer AH, Murphy CA, Cole WJ, Denholm PL. The evolving energy and capacity values of utility-scale PV-plus-battery hybrid system architectures. *Advances in Applied Energy* 2021; 2:100015.
- [21] Liu Z, Wang S, Lim MQ, Kraft M, Wang X. Game theory-based renewable multi-energy system design and subsidy strategy optimization. *Advances in Applied Energy* 2021;2:100024.
- [22] Amabile L, Bresch-Pietri D, Hajje GE, Labbé S, Petit N. Optimizing the self-consumption of residential photovoltaic energy and quantification of the impact of production forecast uncertainties. *Advances in Applied Energy* 2021; 2:100020.

- [23] Wong MS, Zhu R, Liu Z, Lu L, Peng J, Tang Z, Lo CH, Chan WK. Estimation of Hong Kong’s solar energy potential using GIS and remote sensing technologies. *Renewable Energy* 2016;99:325–335.
- [24] Zhu R, Wong MS, You L, Santi P, Nichol J, Ho HC, Lu L, Ratti C. The effect of urban morphology on the solar capacity of three-dimensional cities. *Renewable Energy* 2020;153:1111–1126.
- [25] Catita C, Redweik P, Pereira J, Brito MC. Extending solar potential analysis in buildings to vertical facades. *Computers & Geosciences* 2014;66:1–12.
- [26] Lindberg F, Jonsson P, Honjo T, Wästberg D. Solar energy on building envelopes – 3D modelling in a 2D environment. *Solar Energy* 2015;115:369–378.
- [27] Lobaccaro G, Carlucci S, Croce S, Paparella R, Finocchiaro, L. Boosting solar accessibility and potential of urban districts in the Nordic climate: A case study in Trondheim. *Solar Energy* 2017;149:347–369.
- [28] Peronato G, Rey E, Andersen M. 3D model discretization in assessing urban solar potential: the effect of grid spacing on predicted solar irradiation. *Solar Energy* 2018;176:334–349.
- [29] Zhu R, You L, Santi P, Wong WS, Ratti C. Solar accessibility in developing cities: A case study in Kolwoon East, Hong Kong. *Sustainable Cities and Society* 2019;51:101738.
- [30] Bianchi M, Branchini L, Ferrari C, Melino F. Optimal sizing of grid-independent hybrid photovoltaic–battery power systems for household sector. *Applied Energy* 2014;136:805–816.
- [31] Zhang J, Xua L, Shabunko V, Tay SER, Sun H, Lau SSY, Reindl T. Impact of urban block typology on building solar potential and energy use efficiency in tropical high-density city. *Applied Energy* 2019;240:513–533.
- [32] Zhu R, Wong MS, Kwan MP, Min C, Santi P, Ratti C. An economically feasible optimization of photovoltaic provision using real electricity demand: A case study in New York City. *Sustainable Cities and Society* 2022;78:103614.

- [33] Zhong T, Zhang K, Chen M, Wang Y, Zhu R, Zhang Z, Zhou Z, Qian Z, Lv G, Yan J. Assessment of solar photovoltaic potentials on urban noise barriers using street-view imagery. *Renewable Energy* 2021; 168:181–194.
- [34] Zhong T, Zhang Z, Chen M, Zhang K, Zhou Z, Zhu R, Wang Y, Lv G, Yan J. A City-scale Estimation of Rooftop Solar Photovoltaic Potential Based on Deep Learning. *Applied Energy* 2021; 298:117132.
- [35] Li P, Zhang H, Guo Z, Lyu S, Chen J, Li W, Song X, Shibasaki R, Yan J. Understanding rooftop PV panel semantic segmentation of satellite and aerial images for better using machine learning. *Advances in Applied Energy* 2021; 4:100057.
- [36] Jakubiec JA, Reinhart CF. A method for predicting city-wide electricity gains from photovoltaic panels based on LiDAR and GIS data combined with hourly Daysim simulations. *Solar Energy* 2013;93:127–143.
- [37] Platt SM, Haddad IEL, Pieber SM, Huang RJ, *et al.* Two-stroke scooters are a dominant source of air pollution in many cities. *Nature Communications* 2014;5:3749.
- [38] Tulpule P, Marano V, Yurkovich S, Rizzoni G. Energy economic analysis of PV based charging station at workplace parking garage. *IEEE 2011 EnergyTech* 2011;1–6.
- [39] Fathabadi H. Novel stand-alone, completely autonomous and renewable energy based charging station for charging plug-in hybrid electric vehicles (PHEVs). *Applied Energy* 2020;260:114194.
- [40] Huang P, Ma Z, Xiao L, Sun Y. Geographic Information System-assisted optimal design of renewable powered electric vehicle charging stations in high-density cities. *Applied Energy* 2019;255:113855.
- [41] Tulpule PJ, Marano V, Yurkovich S, Rizzoni G. Economic and environmental impacts of a PV powered workplace parking garage charging station. *Applied Energy* 2013;108:323–332.
- [42] Yan J, Zhang J, Liu Y, Lv G, Han S, Alfonzo IEG. EV charging load simulation and forecasting considering traffic jam and weather to support the integration of renewables and EVs. *Renewable Energy* 2020;159:623–641.

- [43] Kabir ME, Assi C, Tushar MHK, Yan J. Optimal Scheduling of EV Charging at a Solar Power-Based Charging Station. *IEEE Systems Journal* 2020;14(3):4221–4231.
- [44] Islama MS, Mithulananthan N, Hung DQ. Coordinated EV charging for correlated EV and grid loads and PV output using a novel, correlated, probabilistic model. *Electrical Power and Energy Systems* 2019;104:335–348.
- [45] Deshmukh SS, Pearce JM. Electric vehicle charging potential from retail parking lot solar photovoltaic awnings. *Renewable Energy* 2021;169:608–617.
- [46] Figueiredo R, Nunes P, Brito MC. The feasibility of solar parking lots for electric vehicles. *Energy* 2017;140:1182–1197.
- [47] Huang R, Hong F, Ghaderi D. Sliding mode controller-based e-bike charging station for photovoltaic applications. *International Transactions on Electrical Energy Systems* 2020;30:e12300.
- [48] Chandra Mouli GR, Van Duijsen, P, Grazian F, Jamodkar A, Bauer P, Isabella O. Sustainable E-Bike Charging Station That Enables AC, DC and Wireless Charging from Solar Energy. *Energies* 2020;13:3549.
- [49] Mishra S, Dwivedi G, Upadhyay S, Chauhan A. Modelling of standalone solar photovoltaic based electric bike charging. *Materials Today: Proceedings* 2021; <https://doi.org/10.1016/j.matpr.2021.02.738>
- [50] Stasinopoulos S, Zhao M, Zhong, Y. Simultaneous localization and mapping for autonomous bicycles. *International Journal of Advanced Robotic Systems* 2017;14(3):1–16.
- [51] Kondor D, Zhang X, Meghjani M, Santi P, Zhao J, Ratti C. Estimating the potential for shared autonomous scooters. *IEEE Transactions on Intelligent Transportation Systems* 2021;1–12.
- [52] ScooterBee. World’s first on-demand electric scooter, <https://scootbee.com/>; 2021 (accessed 12 December 2021).
- [53] Xu Y, Chen D, Zhang X, Tu W, Chen Y, Shen Y, Ratti C. Unravel the Landscape

- and Pulses of Cycling Activities from A Dockless Bike-Sharing System. *Computers, Environment and Urban Systems* 2019;75:184–203.
- [54] McKenzie G. Spatiotemporal comparative analysis of scooter-share and bike-share usage patterns in Washington, D.C. *Journal of Transport Geography* 2019;78:19–28.
- [55] Cao Z, Zhang X, Chua K, Yu H, Zhao J. E-scooter sharing to serve short-distance transit trips: a Singapore Case. *Transportation Research Part A Policy and Practice* 2021;147:177–196.
- [56] Faghieh-Imani A, Eluru N. Analysing bicycle-sharing system user destination choice preferences: Chicago’s Divvy system. *Journal of Transport Geography* 2015;44:53–64.
- [57] Kaplan S, Manca F, Nielsen TAS, Prato CG. Intentions to use bike-sharing for holiday cycling: An application of the theory of planned behavior. *Tourism Management* 2015;47:34–46.
- [58] Nuzzolo A, Comi A. Individual utility-based path suggestions in transit trip planners. *IET Intelligent Transport Systems* 2016;10(4):219–226.
- [59] Li Z, Zhang J, Gan J, Lu P, Gao Z, Kong W. Large-scale trip planning for bike-sharing systems. *Pervasive and Mobile Computing* 2019;54:16–28.
- [60] Angeloudis P, Hu J, Bell M.G.H. A strategic repositioning algorithm for bicycle-sharing schemes. *Transportmetrica A: Transport Science* 2014;10(8):759–774.
- [61] Ghosh S, Varakantham P, Adulyasak Y, Jaillet P. Dynamic repositioning to reduce lost demand in bike sharing systems. *Journal of Artificial Intelligence Research* 2017;58:387–430.
- [62] Warrington J, Ruchti D. Two-stage stochastic approximation for dynamic rebalancing of shared mobility systems. *Transportation Research Part C* 2019;104:110–134.
- [63] Yoon JW, Pinelli F, Calabrese F. Cityride: a predictive bike sharing journey advisor. *2012 IEEE 13th International Conference on Mobile Data Management* 2012;306–311.

- [64] Meghjani M, Pendleton SD, Marczuk KA, Eng YH, Shen X, Ang MHJ, Rus D. Multi-class Fleet Sizing and Mobility on Demand Service. In *Complex Systems Design & Management Asia 2018* 2018;37–49.
- [65] Sun Earth Tools. Tools for consumers and designers of solar, [https://www.sunearthtools.com/dp/tools/pos\\_sun.php](https://www.sunearthtools.com/dp/tools/pos_sun.php); 2021 (accessed 12 December 2021).
- [66] Huang S, Rich PM, Crabtree RL, Potter CS, Fu P. Modeling Monthly Near-Surface Air Temperature from Solar Radiation and Lapse Rate: Application over Complex Terra in in Yellow stone National Park. *Physical Geography* 2008;29(2):158–178.
- [67] ArcGIS Pro. Points solar radiation, <https://pro.arcgis.com/en/pro-app/latest/tool-reference/spatial-analyst/points-solar-radiation.htm>; 2021 (accessed 12 December 2021).
- [68] Bird. The Bird you can own, <https://one.bird.co/>; 2021 (accessed 12 December 2021).
- [69] OSM. Welcome to OpenStreetMap, <https://www.openstreetmap.org>; 2021 (accessed 12 December 2021).
- [70] PostgreSQL. PostgreSQL: The World’s Most Advanced Open Source Relational Database, <https://www.postgresql.org/>; 2021 (accessed 12 December 2021).
- [71] World Weather. Historical monthly weather, <https://www.worldweatheronline.com>; 2021 (accessed 12 December 2021).
- [72] Kelley LC, Gilbertson E, Sheikh A, Eppinger SD, Dubowsky S. On the feasibility of solar-powered irrigation. *Renewable and Sustainable Energy Reviews* 2010;14:2669–2682.
- [73] KickScooter T60. The world’s first semi-automatic, teleoperating shared scooter, <https://b2b.segway.com/kickscooter-t60/>; 2021 (accessed 12 December 2021).